Etiology of white matter hyperintensities in autosomal dominant and sporadic Alzheimer's disease

Zahra Shirzadi, PhD[1], Stephanie A. Schultz, PhD[1], Wai-Ying W. Yau, MD[1], Nelly Joseph-Mathurin, PhD[2], Colleen D. Fitzpatrick[1], Raina Levin[1], Kejal Kantarci, MD, MS[3], Gregory M. Preboske, MS[3], Clifford R. Jack Jr., MD[3], Martin R. Farlow, MD[4], Jason Hassenstab, PhD[2], Mathias Jucker, PhD[5], John C. Morris, MD[2], Chengjie Xiong, PhD[2], Celeste M. Karch, PhD[2], Allan I. Levey, MD, PhD[6], Brian A. Gordon, PhD[2], Peter R. Schofield, PhD DSc[7], Stephen P. Salloway, MD[8], Richard J. Perrin, MD, PhD[2], Eric McDade, DO[2], Johannes Levin, MD[9], Carlos Cruchaga, PhD[2], Ricardo F. Allegri, MD, PhD[10], Nick C. Fox, MD FRCP FMedSci[11], Alison Goate, PhD[2], Gregory S. Day, MD, MSc[12], Robert Koeppe, PhD[13], Helena C. Chui, MD[14], Sarah Berman, MD, PhD[15], Hiroshi Mori, PhD[16], Raquel Sanchez-Valle, MD, PhD[17], Jae-Hong Lee, MD, PhD[18], Pedro Rosa-Neto, MD, PhD[19], Myuri Ruthirakuhan[20], Che-Yuan Wu, BSc[20], Walter Swardfager, PhD[20], Tammie L.S. Benzinger, MD, PhD[2], Hamid R Sohrabi, PhD[21], Ralph N. Martins, PhD[22], Randall J. Bateman, MD[2], Keith A. Johnson, MD[1], Reisa A. Sperling, MD[1], Steven M. Greenberg, MD, PhD[1], Aaron P. Schultz, PhD[1], Jasmeer P. Chhatwal, MD, PhD, MMSc[1], on behalf of the Dominantly Inherited Alzheimer Network and the Alzheimer's Disease Neuroimaging Initiative

(1) Massachusetts General Hospital, Brigham and Women's Hospital, Harvard Medical School, Boston, MA, USA
(2) Washington University in St. Louis School of Medicine, St. Louis, MO, USA,
(3) Mayo Clinic, Radiology, Rochester, MN, USA,
(4) Indiana Alzheimer's Disease Research Center, Indianapolis, IN, USA,
(5) Department of Cellular Neurology, Hertie Institute for Clinical Brain Research, University of Tübingen, German Center for Neurodegenerative Diseases (DZNE), Tübingen, D-72076 Tübingen, Germany,
(6) Emory University School of Medicine, Atlanta, GA, USA,
(7) Neuroscience Research Australia, Sydney, NSW, Australia; and School of BioMedical Sciences, University of New South Wales, Sydney, NSW, Australia,
(8) Alpert Medical School of Brown University, Providence, RI, USA,
(9) Department of Neurology, Ludwig-Maximilians-Universität München, German Center for Neurodegenerative Diseases, site Munich, Munich Cluster for Systems Neurology (SyNergy), Munich, Germany
(10) Fleni Neurological Institute, Buenos Aires, Argentina,
(11) UK Dementia Research Institute, UCL, London, United Kingdom,
(12) Mayo Clinic, Jacksonville, FL, USA,
(13) University of Michigan, Ann Arbor, MI, USA,

(14) University of Southern California, Los Angeles, CA, USA,
(15) University of Pittsburgh, Pittsburgh, PA, USA,
(16) Osaka Metropolitan University Medical School, Osaka, Nagaoka Sutoku University, Japan,
(17) Neurological Tissue Bank Hospital Clinic, IDIBAPS, Barcelona, Spain,
(18) Asan Medical Center, University of Ulsan College of Medicine, Seoul, Korea, Republic of (South)
(19) Montreal Neurological Institute, McGill University, Montreal, QC, Canada,
(20) Sunnybrook research institute, University of Toronto, ON, Canada
(21) Centre for Healthy Ageing, School of Psychology, Health Future Institute, Murdoch University, Perth, Western Australia, Australia,
(22) School of Medical and Health Sciences, Edith Cowan University, Perth, Western Australia, Australia

Corresponding author

Jasmeer Chhatwal, MD, PhD

MGH Neurology

149 13th St, Room 2662

Charlestown, MA 02129

617-726-1337

Key points (99/100)

Question: Are MRI-visible white matter hyperintesities in Alzheimer's disease (AD) more strongly related to neurodegenerative processes or systemic vascular risk factors?

Findings: In cross-sectional and longitudinal data from both autosomal dominant and late-onset AD cohorts (N = 1141), white matter hyperintesity volume was much more tightly associated with the AD-intrinsic processes of gray matter atrophy, parenchymal and vessel amyloidosis as compared to systemic vascular risk factors.

Meaning: In adults with AD, white matter hyperintesity volume may not reflect the effects of mixed vascular pathology secondary to elevated systemic vascular risk, but rather might be related to amyloidosis and neurodegeneration.

Abstract (345/350)

Importance: Increased volume of white matter hyperintensities (WMH) is a common MRI finding in both autosomal dominant Alzheimer's disease (ADAD) and late-onset Alzheimer's disease (LOAD), but it remains unclear whether these increased WMH are reflective of AD-intrinsic processes or evidence of white-matter damage secondary to elevated systemic vascular risk factors (e.g., small vessel ischemic changes suggestive of mixed vascular and AD pathologies).

Objective: To estimate the contributions of AD-related neurodegeneration, parenchymal, and vessel amyloidosis on WMH accumulation, and to determine if systemic vascular risk adds to WMH beyond these AD-intrinsic processes.

Design: Data from three longitudinal cohort studies were used—the Dominantly Inherited Alzheimer's Network (DIAN), Alzheimer's Disease Neuroimaging Initiative (ADNI), and the Harvard Aging Brain Study (HABS).

Setting: Tertiary and community-based medical centers.

Participants: This study included data from 1141 cognitively impaired and unimpaired individuals (252 pathogenic variant carriers from DIAN; 889 older adults from ADNI and HABS).

Main outcome and measures: We assessed the independent contributions of neurodegeneration (gray matter volume), parenchymal amyloidosis (amyloid PET), vessel amyloidosis (evidenced by cortical microbleeds; CMBs), and systemic vascular risk (Framingham Heart Study cardiovascular disease risk score) on cross-sectional and longitudinal WMH volumes.

Results: We observed that longitudinal increases in WMH volume were: (1) greater in individuals with CMBs compared to those without (DIAN: $t=3.2$, $p=0.001$; ADNI: $t=2.7$, $p=0.008$); (2) associated with longitudinal decreases in gray matter volume (DIAN: $t=-3.1$, $p=0.002$; ADNI: $t=-5.6$, $p<0.001$; HABS: $t=-2.2$, $p=0.03$); (3) greater in older individuals (DIAN: $t=6.8$, $p<0.001$; ADNI: $t=9.1$, $p<0.001$; HABS: $t=5.4$, $p<0.001$); and (4) not significantly correlated with systemic vascular risk in ADAD and LOAD after accounting for age, gray matter volume, CMB presence, and amyloid burden. In older adults without CMBs at baseline, greater

WMH volume was predictive of CMB development during longitudinal follow-up (Cox HR=2.63 (CI:1.72-4.03), p<0.001).

Conclusions and Relevance: Increased WMH volume in AD is associated with the AD-intrinsic processes of neurodegeneration, parenchymal and vessel amyloidosis and may not reflect the effects of elevated systemic vascular risk. Additionally, increased WMH volume may represent an early sign of vessel amyloidosis, preceding the emergence of CMBs.

Introduction:

The finding of increased white matter hyperintensities (WMH) volume on routine magnetic resonance imaging (MRI) in individuals being evaluated for Alzheimer's disease (AD) is both extremely common and vexingly non-specific[1–3]. Increased WMH in the absence of MR-visible strokes or hemorrhage is observed in a wide variety of conditions, ranging from neurodegenerative to inflammatory to cerebrovascular syndromes, reflecting the broad set of possible etiologies that drive WMH appearance and accumulation. WMH are often presumed to represent small-vessel ischemic-brain injury due to underlying vascular risk factors, including hypertension, diabetes, and hyperlipidemia[4]. WMH are also commonly seen in individuals diagnosed with both sporadic, late-onset Alzheimer's disease (LOAD) and autosomal dominant Alzheimer's disease (ADAD)[5–7]. However, despite the consistent finding that many individuals with AD have elevations in WMH volume compared to age-matched controls[8,9] the interpretation of WMH in AD remains controversial. The presence of periventricular WMH is often attributed to traditional cardiovascular risk factors[10]. In older adults and people with LOAD, the presence or absence of WMH is used to support or argue against a diagnosis of mixed vascular and neurodegenerative pathologies as etiologic drivers of cognitive decline. This interpretation of WMH as sequelae of elevated systemic vascular risk has been tremendously influential, forming the basis of clinical recommendations, and informing diagnostic criteria for vascular dementia and vascular cognitive impairment[11].

More recent studies suggest that WMH may also be related to amyloid accumulation and cerebral amyloid angiopathy (CAA)[12,13], though simultaneous assessment of both of these possible drivers of WMH has rarely been performed. CAA is clinically diagnosed by detecting hemorrhagic lesions, most commonly, cerebral microbleeds (CMBs)[14]. However, these hemorrhagic lesions (including CMBs) are a relatively late consequence of vessel amyloidosis, and detection of CAA physiology in the pre-CMB phase of the disease remains challenging. The study of autosomal dominant forms of CAA, in which the disease manifests in relatively young adults with lower levels of systemic vascular risk, shows that white matter injury begins very early in the course of the disease, with WMH growth evident more than a decade prior to the appearance of CMBs or other hemorrhagic lesions[15]. It has also been hypothesized that WMH partly represents a consequence of cortical atrophy and resultant downstream axonal loss it generates[2,16,17].

A major challenge in assessing the etiology of WMH is that multiple potential drivers of WMH growth are often present within an individual, especially in older individuals on the AD continuum. Simultaneously assessing these drivers of WMH growth requires comprehensive imaging and clinical data to be available, including clinical data on vascular risk factors, AD biomarkers, MRI, and PET. In the present study, we leverage multimodal data from three large ADAD and LOAD cohorts that prospectively collected longitudinal measures of vascular, neurodegenerative, and amyloid-related processes to test the hypothesis that WMH in AD may be more strongly associated with AD-intrinsic processes as compared to traditional systemic vascular risk factors.

Material and Methods:

Participants:

Participants provided written, informed consent prior to the performance of any study procedures, as mandated by human subject research committees at each site.

DIAN study: We evaluated 252 participants in the Dominantly Inherited Alzheimer's Network (DIAN) observational study using previously described clinical, neuropsychological, and imaging assessments[18], using data from the 12th DIAN Data Freeze. Individuals bearing the *APP* E693Q (Dutch type CAA) were excluded. All other *APP*, *PSEN1*, and *PSEN2* pathogenic variant carriers with available neuroimaging and clinical data were included. Longitudinal analyses were performed in ADAD carriers with at least one follow-up MRI and clinical visit.

ADNI study: We evaluated 571 individuals from Alzheimer's Disease Neuroimaging Initiative (ADNI1, ADNIGO, ADNI2, ADNI3) with available clinical and neuroimaging data. Baseline clinical diagnoses included: cognitively unimpaired (25%), subjective memory complaint (5%), early mild cognitive impairment (35%), late mild cognitive impairment (22%), and dementia (13%). All included ADNI participants had at least one follow-up MRI visit and clinical data.

HABS study: We evaluated 318 individuals from the Harvard Aging Brain Study (HABS) with available clinical and neuroimaging data. All participants were cognitively unimpaired at study entry and had at least one available follow up visit.

Image acquisition and processing:

MRI: The following MR images (3T) were used: 1) T1-weighted MPRAGE: TR/TE/TI=2300/2.95/900ms, dimensions=1.1×1.1×1.2mm^3, 2) Fluid attenuated recovery (FLAIR): TR/TE/TI=9000/91/2500ms, dimensions=0.86×0.86×5mm^3 or 3D FLAIR: TR/TE/TI=6000/454/2100ms, dimensions=1×1×1.5mm^3, and 3) Susceptibility weighted MRI: TR/TE=28/20ms, dimensions=0.7×0.7×2.4mm^3 or T2*-weighted gradient echo weighted MRI: TR/TE=650/20ms, dimensions=0.8×0.8×4mm^3.

We segmented WMH on FLAIR images using the HyperMapp3r algorithm (https://hypermapp3r.readthedocs.io/). HyperMapp3r is a convolutional neural network-based segmentation algorithm that uses T1-weighted, FLAIR, and brain mask images to generate WMH predictions in the subject space[19]. For illustration purposes, WMH masks were co-registered to MNI standard space using the FLIRT tool (https://fsl.fmrib.ox.ac.uk/fsl/fslwiki/FLIRT) in FSL6.0.1. Subsequently, a map indicating the probability of recognizing WMH in a given voxel was generated using baseline data (WMH probability map) in order to visualize the patterns and volume of WMH in different groups.

Gray matter (GM) volume and intracranial volume were assessed using FreeSurfer (https://surfer.nmr.mgh.harvard.edu/)[20]. WMH and GM volume were normalized to intracranial volume prior to entry into models. Normalized WMH volume was log-transformed to reduced skewness. Lobar CMB burden was assessed visually on susceptibility-weighted/T2*-weighted gradient echo images by experienced radiologists at the Mayo Clinic in Rochester for DIAN and ADNI[21] and at the Masschusets General Hospital for HABS[22]. Small lesions (≤10mm) that were dissociable from small vessels were counted as definite microbleeds.

Amyloid PET: Detailed amyloid PET protocols have been previously described for DIAN[23], ADNI[24], and HABS[25]. Amyloid PET was performed using C^{11}– Pittsburgh Compound B (PiB) in DIAN and HABS and F^{18}–florbetapir (FBP) in ADNI. In ADNI, florbetapir measurements were represented as a cortical summary standard uptake value ratio (SUVr) across a composite of lateral and medial frontal, anterior, and posterior cingulate, lateral parietal, and lateral temporal regions. The whole cerebellum served as the reference region. Data, including information on dichotimization of amyloid groups based on FBP-PET, were downloaded from the LONI website for ADNI participants (http://adni.loni.usc.edu/). As in prior work from

HABS[26], PiB PET measurements were represented as a distribution volume ratio across a composite of frontal, lateral temporal, parietal, and retrosplenial regions, with cerebellar gray matter serving as the reference region. As in ADNI, HABS participants were grouped into high and low amyloid groups using previously-described, cohort specific cutoff values. Similar processing was performed in DIAN and we obtained cortical mean SUVr values from PiB PET. As the application of LOAD-based thresholds for amyloid positivity in ADAD may be complicated by variant-level differences in amyloid PET signal, PiB SUVr was used as a continuous variable in DIAN analyses[27].

Statistical analyses:

Statistical testing was conducted in R v4.0.2 (R Foundation for Statistical Computing). Cross-sectional models used linear regression to examine the association of CMBs (presence/absence), GM volume, and age with WMH volume at baseline. Interactions of amyloid group with gray matter volume were examined and retained only if statistically significant. Follow-up sensitivity analyses examined the potentially additive effect of an algorithmic vascular risk score (Framingham Heart Study Cardiovascular Disease risk score (FHS-CVD)[28]) in the model. Lastly, to assess how relationships between CMBs, GM, and age on WMH volumes may change in the higher ranges of systemic vascular risk, cross-sectional models were re-run in the highest tertile of FHS-CVD for each cohort.

For longitudinal analyses WMH and GM volume rates of change were extracted from linear mixed-effects models (lme4 package), and associations between CMBs (presence/absence), GM volume rate of change, and age with WMH volume rate of change were assessed. As in cross-sectional analyses, the interaction of amyloid group and gray matter volume was assessed and retained if significant. Paralleling cross-sectional analyses, follow-up sensitivity analyses were performed to assess baseline FHS-CVD as a predictor of WMH rate of change, as well as in analyses restricted to the highest tertile of FHS-CVD in each cohort. Lastly, to assess the relationship between baseline WMH burden and the development of CMB during longitudinal follow-up, a survival analysis (survival package) was performed. Survival curves were depicted using the Kaplan-Meier method.

Results:

Table 1 summarizes the clinical characteristics of DIAN, ADNI, and HABS cohorts used in primary analyses. Supplementary Table 1 summarizes the clinical characteristics of the highest tertile of FHS-CVD groups in DIAN, ADNI, and HABS – a subgroup used in sensitivity analyses (Supplemental Tables 2-7) in which the statistical analyses were restricted to those individuals with the highest levels of systemic vascular risk within their study cohort.

DIAN study: Baseline WMH volume was greater in ADAD pathogenic variant carriers who had at least one baseline CMB ($t=2.1$, $p=0.03$; Figure 1A), who were older in age (i.e., closer to their estimated age of symptom onset; $t=4.7$, $p<0.001$) and who had lower GM volume ($t=-2.3$, $p=0.02$; Figure 1B; Figure 2A). Sensitivity analyses indicated that including the FHS-CVD score as a predictor did not change the associations between WMH, age, and GM volume, but slightly attenuated the effect of CMB on WMH volume (Supplementary Table 2). Systemic vascular risk as assessed using the FHS-CVD score was not associated with cross-sectional WMH volume. Similar associations between CMB and GM volume with WMH were observed when restricting analyses to participants with higher levels of vascular risk (highest tertile of FHS-CVD for this cohort; Supplementary Table 2).

We next examined the associations between WMH volume and GM volume, CMB presence, and amyloid PET signal in ADAD longitudinal data. Longitudinal increases in WMH amongst ADAD pathogenic variant carriers with CMB were greater than amongst carriers without CMB ($t=3.2$, $p=0.001$). In addition, higher GM volume rate of change ($t=-3.1$, $p=0.002$) was associated with increasing WMH volume in longitudinal MRI data (Figure 2B). FHS-CVD did not alter the associations between CMB, amyloid burden, and GM atrophy with longitudinal WMH volume (Supplementary Table 3). Associations between age and GM volume rate of change with WMH rate of change remained similar when restricting the analysis to participants in the highest tertile of FHS-CVD for the cohort, but CMB associations with WMH rate-of-change became non-significant (Supplementary Table 3).

ADNI study: We next examined whether similar associations between amyloidosis and GM volume with WMH volume were observable in older adults from ADNI. Similar to results in ADAD, cross-sectional WMH volume was greater in older adults with CMB vs. those without ($t=2.3$, $p=0.02$; Figure 1A). We also observed that WMH volume was strongly associated with

GM volume (t=-6.8, p<0.001; Figure 1B), older age (t=10.5, p<0.001, Figure 3A), and higher levels of amyloid burden (t=2.2, p = 0.03; Figure 1C). Including FHS-CVD in cross-sectional models did not alter the associations of GM volume and age with WMH, but the effects of CMB and amyloid group on cross-sectional WMH became non-significant in these models. FHS-CVD itself was not associated with cross-sectional WMH after accounting for GM volume, CMB, and age. We observed similar results when analyses were restricted to ADNI participants in the highest tertile of FHS-CVD (Supplementary Table 4).

Consonant patterns of association were observed in longitudinal data from ADNI. Specifically, older adults with CMB demonstrated greater longitudinal increases in WMH volume compared to those without CMB (t=2.7, p=0.008). Longitudinal WMH growth was strongly associated with progressive GM atrophy (t=-5.6, p<0.001), older age (t=9.1, p<0.001), and amyloid positivity (t=2.3, p=0.02, Figure 3B). Including FHS-CVD score as a predictor or restricting the analysis to only individuals in the highest tertile of FHS-CVD weakened associations between amyloid grouping and WMH rate-of-change, but did not alter associations between CMB, GMV rate of change, and age with WMH rate-of-change. Additionally, FHS-CVD itself was not related to WMH volume rate of change. (Supplementary Table 5).

HABS study: We next examined whether associations between CMB, amyloid burden, and GM volume with WMH volume were observable in data from older adults participating in HABS, all of whom entered the study cognitively unimpaired. Similar to results in ADNI and DIAN, WMH volume in HABS participants was greater in older adults with CMB vs. those without (t=2.2, p=0.02; Figure 1A). WMH volume was also associated with the interaction of GM volume and amyloid group (t=-2.1, p=0.04; Figure 1B; Figure 1C) and older age (t=5.4, p<0.001; Figure 4A). Including the FHS-CVD score did not alter the associations of GM volume and age with WMH, but did attenuate the association of CMB with WMH (Supplementary Table 6). When restricting the analysis to the highest FHS-CVD tertile group from HABS, cross-sectional WMH volume was only related to older age (Supplementary Table 6).

Similar to cross-sectional analyses, the interaction of amyloid group and GM volume rate of change was significantly associated with WMH rate-of-change (t=-2.2, p=0.03, Figure 4B) in longitudinal analyses. Follow-up sensitivity analyses including FHS-CVD as a predictor demonstrated a trend-level association between baseline FHS-CVD and WMH rate-of-change (t=1.8, p=0.06), with other effects unchanged. Restricting the analysis to HABS participants in

the highest tertile of FHS-CVD, WMH volume rate of change was significantly related only to older age (Supplementary Table 7). Notably, the effect of CMB was omitted in longitudinal analyses from HABS, as longitudinal data on CMBs in HABS participants (beyond study baseline) were not available.

Survival analysis in ADNI: Lastly, building on the observation that individuals with increased WMH volume were more likely to have CMBs at study entry, we examined whether a higher baseline WMH burden was predictive of the emergence of CMBs during longitudinal follow-up in ADNI participants who did not have CMBs at baseline (n=527). Of these 527 participants, 100 individuals (19%) developed at least one CMB during follow-up visits (CMB emergent group, Supplementary Table 8). Individuals with WMH volume above the median at baseline had a higher risk of developing CMB during follow-up visits (hazard ratio=2.63 (95% confidence interval = 1.72 to 4.03), $p<0.001$; Figure 5), after controlling for age and GM volume. Including FHS-CVD risk score and amyloid burden did not alter these findings.

Discussion

While increased WMH are a common MRI finding in individuals on an AD trajectory, the interpretation and diagnostic implications of elevated WMH volume in AD remain ambiguous due to the potential influence of a broad set of vascular and neurodegenerative factors on WMH growth. While WMH in AD are often interpreted in the context of small vessel ischemic changes secondary to systemic vascular risk factors (mixed vascular pathology), the findings here suggest that WMH are related to the AD-intrinsic processes of parenchymal and vessel amyloidosis (i.e., CAA) and degeneration of cerebral gray matter more so than to traditional systemic vascular risk factors. These findings are supported by the examination of three complementary datasets with available AD biomarkers, clinical data, and longitudinal neuroimaging data: a relatively young cohort with high rates of AD-related GM atrophy and CAA, low vascular risk, and limited potential for other, non-AD age-related pathologies (ADAD carriers in the DIAN cohort); and two cohorts of older adults with roughly average levels of vascular risk for their age, some with preclinical or symptomatic LOAD, and higher potential for co-morbid, non-AD pathologies[29] (data from ADNI and HABS). In all cohorts examined, the presence of CMBs (indicative of possible CAA physiology) and lower gray matter volume (a broad-based measure of neurodegeneration) were independently related to greater baseline

WMH volumes. The presence of CMBs and GM atrophy were also independently related to higher longitudinal rates of change in WMH volume in both ADAD and LOAD cohorts, concordant with cross-sectional results. Additionally, we observed that higher WMH volumes in older adults from ADNI *without* CMBs at baseline were predictive of the development of CMBs during longitudinal follow-up, suggesting that increasing WMH volume may reflect progressive vessel amyloidosis even before MRI-visible CMBs are manifest. Consistent with this possibility, longitudinal rates of WMH change were higher in individuals with higher amyloid burden, even after controlling for the presence of CMBs and the effects of GM atrophy effects on WMH. In contrast, systemic vascular risk factors (operationalized using the FHS-CVD, a well-validated algorithmic risk score) were poorly correlated with cross-sectional and longitudinal WMH volumes in ADAD and LOAD after controlling for the effects of age, GM atrophy, amyloid burden, and the presence of CMBs.

Together these findings suggest that elevated WMH volume in ADAD and LOAD should be considered in the larger context of neurodegeneration and as a possible reflection of CAA progression – even in individuals without manifest CMBs. These findings also argue that AD-related processes – parenchymal amyloidosis, vessel amyloidosis, and neurodegeneration –may account for a large proportion of the increased WMH volume seen in AD and that the presence of elevated WMH in AD patients may not necessarily reflect the presence of mixed vascular and AD pathologies. Conversely, these findings also suggest that the absence of elevated WMH in older adults with elevated systemic vascular risk should not necessarily strongly decrease suspicion of vascular contributions to cognitive decline.

The observation here that progressive CAA pathophysiology may drive worsening WMH is consistent with recent work from our group and others that have examined white matter disruption in autosomal dominant, Dutch-type CAA due to the *APP* E693Q missense mutation. This prior work in Dutch-type CAA clearly demonstrates that white matter injury is readily observable a decade or more prior to the emergence of CMBs or symptomatic hemorrhage in this population[15]. This was seen in both cross-sectional and longitudinal data from Dutch-type CAA carriers, similar to what was observed here in ADAD carriers and in older adults from ADNI and HABS.

Strikingly, systemic vascular risk was not significantly associated with cross-sectional or longitudinal WMH volume after accounting for age, the presence of CMBs, amyloid burden, and GM atrophy. Though the lack of strong or independent associations between vascular risk and WMH burden is somewhat surprising, this result is consistent with prior reports that vascular risk factors explain only 1-2% of the variance in WMH[30,31]. The presence and clear progression of WMH in autosomal dominant AD and Dutch-type CAA[15,32] – both relatively young populations with low levels of vascular risk – provides a unique channel of evidence that amyloid-related disease processes promote WMH, even in the relative absence of elevated systemic vascular risk. Notably, the pattern of results seen here is consistent with neuropathological studies demonstrating poor associations between WMH volume and vascular risk factors, and stronger relationships to AD pathology - especially prior work that demonstrates WMH are closely related to elevated amyloid burden in older adults[13,33].

Importantly, the difference in effect sizes between age, GM atrophy, amyloid burden, and CMBs associations with WMH volume accumulation needs to be interpreted with caution as CMBs (and amyloid in ADNI and HABS) were modeled as a categorical variables, diminishing their statistical power relative to GM volume, which was modeled as a continuous variable. More importantly, since the emergence of CMBs is a relatively late and stochastic event in the progression of CAA, it is likely that many individuals in the CMB-negative group have latent CAA physiology that has not (yet) manifested as CMB or symptomatic hemorrhage. Indeed, we observed that ~19% of the individuals from ADNI who did not have CMB at baseline developed CMB throughout the follow-up of this study (average=3.7 years). The potential for latent CAA physiology in the CMB negative group cannot itself account for the significant association between CMBs and WMHs seen here, but it may diminish the strength of this already strong association.

Certain additional limitations need to be considered in interpreting the results of this study. We did not include tau burden in our analyses as baseline tau PET imaging was not available in many participants across all three cohorts. Although cross-sectional data show no associations between WMH and tau burden[33], future research is needed to investigate the role of tau accumulation on WMH accumulation given the established relationship between tau accumulation and the rate of GM atrophy[34,35]. Importantly, these results and conclusions need to be considered in the context of the study populations included here and their level of vascular

risk. As expected, the relatively young participants in DIAN (average age = 38.3 years) had low levels of vascular risk[36]. Older participants in ADNI and HABS had roughly average vascular risk for their age[37], and therefore had substantial potential to show correlations between systemic vascular and WMH. However, both ADNI and HABS likely under-represent individuals in the highest range of vascular risk. This is an issue common to many longitudinal studies of cognitive aging and AD, as advanced or unstable cardiac conditions, symptomatic stroke, and poorly controlled diabetes are often considered exclusionary for long-term, AD-focused longitudinal studies. While we partially address this limitation by performing follow-up sensitivity analyses in which only individuals in the highest tertile of vascular risk are included (thereby enriching for high levels of vascular risk), we acknowledge that these analyses will need to be repeated in longitudinal AD cohorts selected to have high vascular risk - especially higher rates of type 2 diabetes. Similarly, both the ADNI and HABS cohorts are comprised largely of white Caucasian individuals[38], and therefore, it remains possible that associations between WMH and systemic vascular risk factors will be seen more clearly in study populations with greater representation of certain ethnic or racial groups. On a related note, further work is needed to address the possibility that certain spatial patterns of WMHs (e.g., sub- or juxtacortical) will demonstrate stronger associations with vascular risk as opposed to AD-intrinsic processes, particularly in cohorts enriched for higher vascular risk and/or with lower levels of AD pathology. Accordingly, the results of the present study are best interpreted in the context of AD, and may not generalize to non-AD populations, including those with very high vascular risk.

Despite these limitations, the results of the present study strongly suggest that the AD-related processes of brain amyloidosis and neurodegeneration may outpace vascular risk as driving factors for the increased white matter changes that have been consistently described in ADAD and LOAD. After accounting for these AD-related processes, the lack of association between vascular risk and WMHs further suggests that we should use caution in interpreting the presence or absence of increased WMH volume in AD patients as strong evidence for or against the presence of "mixed" cerebrovascular pathology. Importantly, these data support the further development of white matter centric measures to serve as biomarkers in both AD and CAA. Optimized white matter biomarkers may be particularly useful as measures of vessel amyloidosis in the pre-CMB and pre-hemorrhage phases of CAA, as tools for the study of this early phase of CAA-related pathologic change are largely lacking.

Data sharing statement:

The data used in this study were obtained from DIAN, ADNI, and HABS. DIAN, ADNI, and HABS are publicly available datasets that can be accessed upon request.

Acknowledgments:

Data used in preparation of this article were obtained from the Alzheimer's Disease Neuroimaging Initiative (ADNI) database (adni.loni.usc.edu). As such, the investigators within the ADNI contributed to the design and implementation of ADNI and/or provided data but did not participate in analysis or writing of this report. A complete listing of ADNI investigators can be found at: http://adni.loni.usc.edu/wp-content/uploads/how_to_apply/ADNI_Acknowledgement_List.pdf

Data collection and sharing for this project was funded by the Alzheimer's Disease Neuroimaging Initiative (ADNI) (National Institutes of Health Grant U01 AG024904) and DOD ADNI (Department of Defense award number W81XWH-12-2-0012). ADNI is funded by the National Institute on Aging, the National Institute of Biomedical Imaging and Bioengineering, and through generous contributions from the following: AbbVie, Alzheimer's Association; Alzheimer's Drug Discovery Foundation; Araclon Biotech; BioClinica, Inc.; Biogen; Bristol-Myers Squibb Company; CereSpir, Inc.; Cogstate; Eisai Inc.; Elan Pharmaceuticals, Inc.; Eli Lilly and Company; EuroImmun; F. Hoffmann-La Roche Ltd and its affiliated company Genentech, Inc.; Fujirebio; GE Healthcare; IXICO Ltd.; Janssen Alzheimer Immunotherapy Research & Development, LLC.; Johnson & Johnson Pharmaceutical Research & Development LLC.; Lumosity; Lundbeck; Merck & Co., Inc.; Meso Scale Diagnostics, LLC.; NeuroRx Research; Neurotrack Technologies; Novartis Pharmaceuticals Corporation; Pfizer Inc.; Piramal Imaging; Servier; Takeda Pharmaceutical Company; and Transition Therapeutics. The Canadian Institutes of Health Research is providing funds to support ADNI clinical sites in Canada. Private sector contributions are facilitated by the Foundation for the National Institutes of Health (www.fnih.org). The grantee organization is the Northern California Institute for Research and Education, and the study is coordinated by the Alzheimer's Therapeutic Research Institute at the University of Southern California. ADNI data are disseminated by the Laboratory for Neuro Imaging at the University of Southern California.

DIAN data/image/tissue collection and sharing was supported by the Dominantly Inherited Alzheimer Network (DIAN, U19AG032438) funded by the National Institute on Aging (NIA), the German Center for Neurodegenerative Diseases (DZNE), Institute for Neurological Research (FLENI), the Research and Development Grants for Dementia from Japan Agency for Medical Research and Development, AMED NP21dk0207049 and NIHR UCL/UCLH Biomedical Research Centre and the MRC Dementias Platform UK (MR/L023784/1 and MR/009076/1).

This work was supported by the National Institute of Neurologic Diseases and Stroke (R01NS070834) and the National Institute on Aging (Dominantly Inherited Alzheimer's Network - UF1AG032438; The Harvard Aging Brain Study - P01AG036694; RF1AG079569). Zahra Shirzadi gratefully acknowledges a fellowship award from the Alzheimer's Society of Canada and ADNI engagement core that supported this work. Lastly, data collection for this study was supported by the National Health and Medical Research Council grant (APP1129627) to Ralph N. Martins.

This research was carried out in part at the Athinoula A. Martinos Center for Biomedical Imaging at the Massachusetts General Hospital, using resources provided by the Center for Functional Neuroimaging Technologies, P41EB015896, a P41 Biotechnology Resource Grant supported by the National Institute of Biomedical Imaging and Bioengineering (NIBIB), National Institutes of Health. This work also involved the use of instrumentation supported by the NIH Shared Instrumentation Grant Program and/or High-End Instrumentation Grant Program; specifically, grant numbers S10RR021110, S10RR023401, and S10RR023043.

Potential conflict of interests

There are no conflicts of interest relevant to the content of this study.

Author contributions

Zahra Shirzadi: conception and design of the study, analysis of data, drafting the text or preparing the figures.
Stephanie A. Schultz: analysis of data
Wai-Ying W. Yau: analysis of data
Nelly Joseph-Mathuri: acquisition and analysis of data
Colleen D. Fitzpatrick: acquisition of data
Raina Levin: acquisition of data
Kejal Kantarci: acquisition and analysis of data
Gregory M. Preboske: acquisition and analysis of data
Clifford R. Jack Jr.: conception and design of the study, analysis of data
Martin R. Farlow: acquisition of data
Jason Hassenstab: acquisition of data
Mathias Jucker: acquisition of data
John C. Morris: acquisition of data
Chengjie Xiong: acquisition of data
Celeste M. Karch: acquisition of data
Allan I. Levey: acquisition of data
Brian A. Gordon: analysis of data, drafting the text or preparing the figures.
Peter R. Schofield: acquisition of data
Stephen P. Salloway: acquisition of data
Richard J. Perrin: acquisition of data
Eric McDade: acquisition of data
Johannes Levin: acquisition of data
Carlos Cruchaga: acquisition of data
Ricardo F. Allegri: acquisition of data
Nick C. Fox: acquisition of data
Alison Goate: acquisition of data
Gregory S. Day: acquisition of data, drafting the text or preparing the figures.
Robert Koeppe: acquisition of data
Helena C. Chui: acquisition of data
Sarah Berman: acquisition of data
Hiroshi Mori: acquisition of data
Raquel Sanchez-Valle: acquisition of data
Jae-Hong Lee: acquisition of data
Pedro Rosa-Neto: acquisition of data
Myuri Ruthirakuhan: analysis of data
Che-Yuan Wu: analysis of data
Walter Swardfager: analysis of data
Tammie L.S. Benzinger: analysis and acquisition of data
Hamid R Sohrabi: acquisition of data
Ralph N Martins: acquisition of data
Randall J. Bateman: acquisition of data
Keith A. Johnson: conception and design of the study
Reisa Sperling: conception and design of the study
Steven M. Greenberg: conception and design of the study
Aaron P. Schultz: analysis of data, drafting the text or preparing the figures.
Jasmeer P. Chhatwal: conception and design of the study, analysis of data, drafting the text or preparing the figures.

References:

1. Smith, E. E. What Turns the White Matter White? Metabolomic Clues to the Origin of Age-Related Cerebral White Matter Hyperintensities. *Circulation* **145**, 1053–1055 (2022).
2. McAleese, K. E. *et al.* Frontal white matter lesions in Alzheimer's disease are associated with both small vessel disease and AD-associated cortical pathology. *Acta Neuropathol. (Berl.)* **142**, (2021).
3. McAleese, K. E. *et al.* Parietal white matter lesions in Alzheimer's disease are associated with cortical neurodegenerative pathology, but not with small vessel disease. *Acta Neuropathol. (Berl.)* **134**, 459–473 (2017).
4. Ungvari, Z. *et al.* Hypertension-induced cognitive impairment: from pathophysiology to public health. *Nat. Rev. Nephrol.* **17**, 639–654 (2021).
5. Schoemaker, D. *et al.* White matter hyperintensities are a prominent feature of autosomal dominant Alzheimer's disease that emerge prior to dementia. *Alzheimers Res. Ther.* **14**, 89 (2022).
6. Araque Caballero, M. Á. *et al.* White matter diffusion alterations precede symptom onset in autosomal dominant Alzheimer's disease. *Brain* **141**, 3065–3080 (2018).
7. Lee, S. *et al.* White matter hyperintensities are a core feature of Alzheimer's disease: Evidence from the dominantly inherited Alzheimer network: White Matter Hyperintensities in Familial AD. *Ann. Neurol.* **79**, 929–939 (2016).
8. McAleese, K. E. *et al.* Cortical tau load is associated with white matter hyperintensities. *Acta Neuropathol. Commun.* **3**, 60 (2015).
9. Yoshita, M. *et al.* Extent and distribution of white matter hyperintensities in normal aging, MCI, and AD. *Neurology* **67**, 2192–2198 (2006).

10. Sharma, R., Sekhon, S. & Cascella, M. White Matter Lesions. in *StatPearls* (StatPearls Publishing, 2022).
11. Wardlaw, J. M., Valdés Hernández, M. C. & Muñoz-Maniega, S. What are white matter hyperintensities made of? Relevance to vascular cognitive impairment. *J. Am. Heart Assoc.* **4**, 001140 (2015).
12. Thal, D. R., Ghebremedhin, E., Orantes, M. & Wiestler, O. D. Vascular Pathology in Alzheimer Disease: Correlation of Cerebral Amyloid Angiopathy and Arteriosclerosis/Lipohyalinosis with Cognitive Decline. *J. Neuropathol. Exp. Neurol.* **62**, (2003).
13. Pålhaugen, L. *et al.* Brain amyloid and vascular risk are related to distinct white matter hyperintensity patterns. *J. Cereb. Blood Flow Metab.* **41**, 1162–1174 (2021).
14. Caetano, A., Ladeira, F., Barbosa, R., Calado, S. & Viana-Baptista, M. Cerebral amyloid angiopathy – The modified Boston criteria in clinical practice. *J. Neurol. Sci.* **384**, 55–57 (2018).
15. Shirzadi, Z. *et al.* Progressive White Matter Injury in Preclinical Dutch Cerebral Amyloid Angiopathy. *Ann. Neurol.* (2022) doi:10.1002/ana.26429.
16. McAleese, K. E. *et al.* Parietal white matter lesions in Alzheimer's disease are associated with cortical neurodegenerative pathology, but not with small vessel disease. *Acta Neuropathol. (Berl.)* **134**, (2017).
17. Leys, D. *et al.* Could Wallerian degeneration contribute to 'leuko-araiosis' in subjects free of any vascular disorder? *J. Neurol. Neurosurg. Psychiatry* **54**, (1991).
18. Morris, J. C. *et al.* Developing an international network for Alzheimer's research: the Dominantly Inherited Alzheimer Network. *Clin. Investig.* **2**, (2012).

19. Mojiri Forooshani, P. *et al.* Deep Bayesian networks for uncertainty estimation and adversarial resistance of white matter hyperintensity segmentation. *Hum. Brain Mapp.* **43**, 2089–2108 (2022).
20. Reuter, M., Schmansky, N. J., Rosas, H. D. & Fischl, B. Within-subject template estimation for unbiased longitudinal image analysis. *NeuroImage* **61**, (2012).
21. Kantarci, K. *et al.* Focal hemosiderin deposits and beta-amyloid load in the ADNI cohort. *Alzheimers Dement.* **9**, (2013).
22. Fotiadis, P. *et al.* Cortical atrophy in patients with cerebral amyloid angiopathy: a case-control study. *Lancet Neurol.* **15**, 811–819 (2016).
23. Su, Y. *et al.* Quantitative Amyloid Imaging in Autosomal Dominant Alzheimer's Disease: Results from the DIAN Study Group. *PLOS ONE* **11**, e0152082 (2016).
24. Jagust, W. J. *et al.* The Alzheimer's Disease Neuroimaging Initiative 2 PET Core: 2015. *Alzheimers Dement. J. Alzheimers Assoc.* **11**, 757–771 (2015).
25. Rabin, J. S. *et al.* Interactive Associations of Vascular Risk and β-Amyloid Burden With Cognitive Decline in Clinically Normal Elderly Individuals: Findings From the Harvard Aging Brain Study. *JAMA Neurol.* **75**, 1124–1131 (2018).
26. Yau, W.-Y. W. *et al.* Tau mediates synergistic influence of vascular risk and Aβ on cognitive decline. *Ann. Neurol.* (2022) doi:10.1002/ana.26460.
27. Chhatwal, J. P. *et al.* Variant-dependent heterogeneity in amyloid β burden in autosomal dominant Alzheimer's disease: cross-sectional and longitudinal analyses of an observational study. *Lancet Neurol.* **21**, 140–152 (2022).
28. D'Agostino, R. B. *et al.* General cardiovascular risk profile for use in primary care: the Framingham Heart Study. *Circulation* **117**, 743–753 (2008).

29. Cairns, N. J. *et al.* Neuropathologic assessment of participants in two multi-center longitudinal observational studies: the Alzheimer Disease Neuroimaging Initiative (ADNI) and the Dominantly Inherited Alzheimer Network (DIAN). *Neuropathol. Off. J. Jpn. Soc. Neuropathol.* **35**, 390–400 (2015).
30. Sliz, E. *et al.* Circulating Metabolome and White Matter Hyperintensities in Women and Men. *Circulation* **145**, (2022).
31. Wardlaw, J. M. *et al.* Vascular risk factors , large-artery atheroma , and brain white matter hyperintensities. *Neurology* **82**, 1331–1338 (2014).
32. Lee, S. *et al.* White matter hyperintensities are a core feature of Alzheimer's disease: Evidence from the dominantly inherited Alzheimer network. *Ann. Neurol.* **79**, (2016).
33. Graff-Radford, J. *et al.* White matter hyperintensities: Relationship to amyloid and tau burden. *Brain* **142**, (2019).
34. Scott, M. R. *et al.* Inferior temporal tau is associated with accelerated prospective cortical thinning in clinically normal older adults. *NeuroImage* **220**, 116991 (2020).
35. Sepulcre, J. *et al.* In Vivo Tau, Amyloid, and Gray Matter Profiles in the Aging Brain. *J. Neurosci. Off. J. Soc. Neurosci.* **36**, 7364–7374 (2016).
36. Joseph-Mathurin, N. *et al.* Longitudinal Accumulation of Cerebral Microhemorrhages in Dominantly Inherited Alzheimer Disease. *Neurology* **96**, (2021).
37. Marma, A. K. & Lloyd-Jones, D. M. Systematic Examination of the Updated Framingham Heart Study General Cardiovascular Risk Profile. *Circulation* **120**, 384–390 (2009).
38. Ashford, M. T. *et al.* Screening and enrollment of underrepresented ethnocultural and educational populations in the Alzheimer's Disease Neuroimaging Initiative (ADNI). *Alzheimers Dement. J. Alzheimers Assoc.* **18**, 2603–2613 (2022).

Table 1: Participants' demographics and study information for the DIAN, ADNI, and HABS baseline data. Mean (Standard deviation) or number (percentage) are reported.

	DIAN (N=252)	**ADNI (N=571)**	**HABS (N=318)**
Age (years)	38.4 (11.2)	72.8 (7.3)	72.4 (7.6)
Estimated year to symptom onset (years)	-8.3 (11.3)	NA	NA
APOE e4 (yes)	74 (29%)	270 (47%)	87 (28%)
Sex (Female)	137 (54%)	274 (48%)	194 (61%)
Education (years)	14 (3)	16 (3)	16 (3)
Cerebral microbleed (yes)	24 (9.5)	44 (8%)	74 (27%)
CDR (1+)	78 (31%)	328 (57%)	3 (1%)
Diagnostic group (dementia)	46 (18%)	74 (13%)	0 (0%)
Amyloid group (high)	NA	274 (50%)	119 (38%)
WMH volume (normalized to ICV=1300cm^3)	2 (6)	9 (9)	5.4 (8.5)
GM volume (normalized to ICV=1300cm^3)	534 (46)	360 (29)	500 (27)
Follow-up time (years)	2.7 (2.5)	3.7 (2.8)	5.2 (3.7)
FHS-CVD score	4.9 (5.1)	38 (22)	30 (18)

NA: not applicable

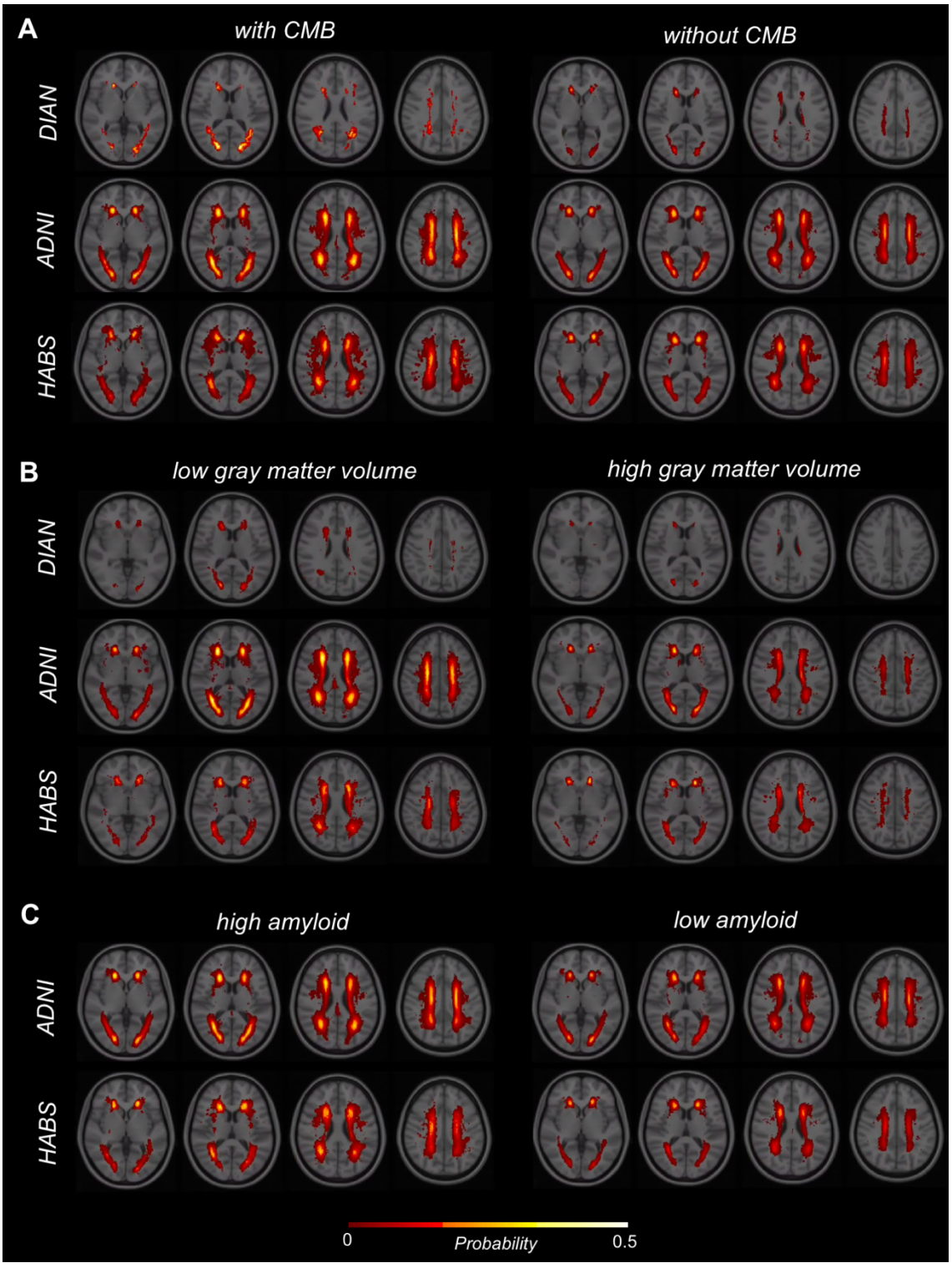

Figure 1: WMH probability maps for a visual illustration of the spatial distribution of WMH in the three cohorts of DIAN, ADNI, and HABS in individuals with and without CMB (A), low and high gray matter volume (B), and low and high amyloid burden (C) at baseline. Individual WMH maps were co-registered to MNI space to generate these probability maps.

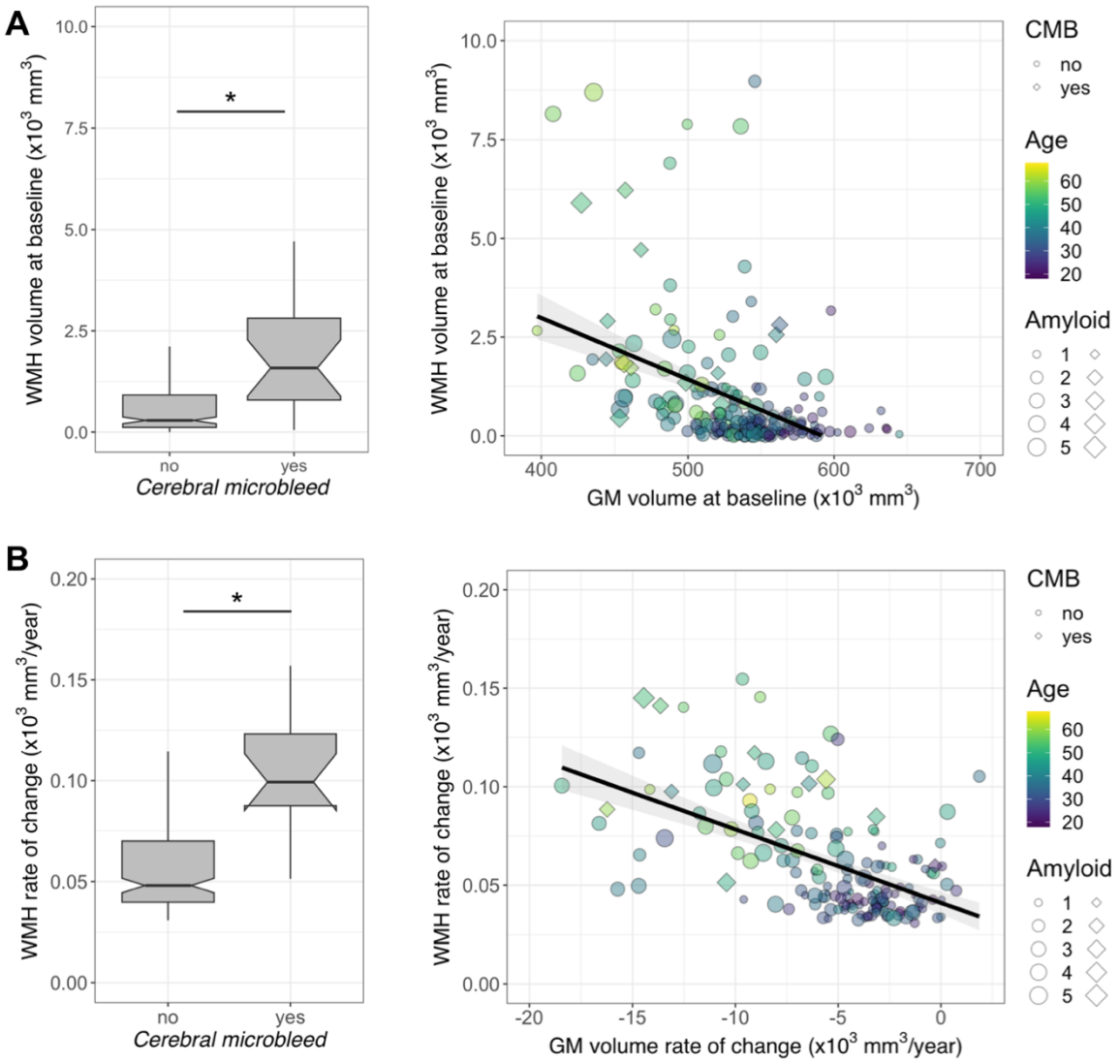

Figure 2: Cerebral microbleeds (CMB) and gray matter (GM) volume are associated with WMH volume in ADAD mutation carriers, both at baseline (A) and longitudinally (B). Carriers with CMB were observed to have greater WMH volume at baseline (top left) and had greater rates of longitudinal WMH volume growth (bottom left) compared to carriers without CMB. In addition, WMH volume was greater in ADAD carriers with lower GM volume (top right). WMH volume growth was correlated with declining GM volume in longitudinal MRI imaging from ADAD carriers (bottom right).

**: $p<0.5$*

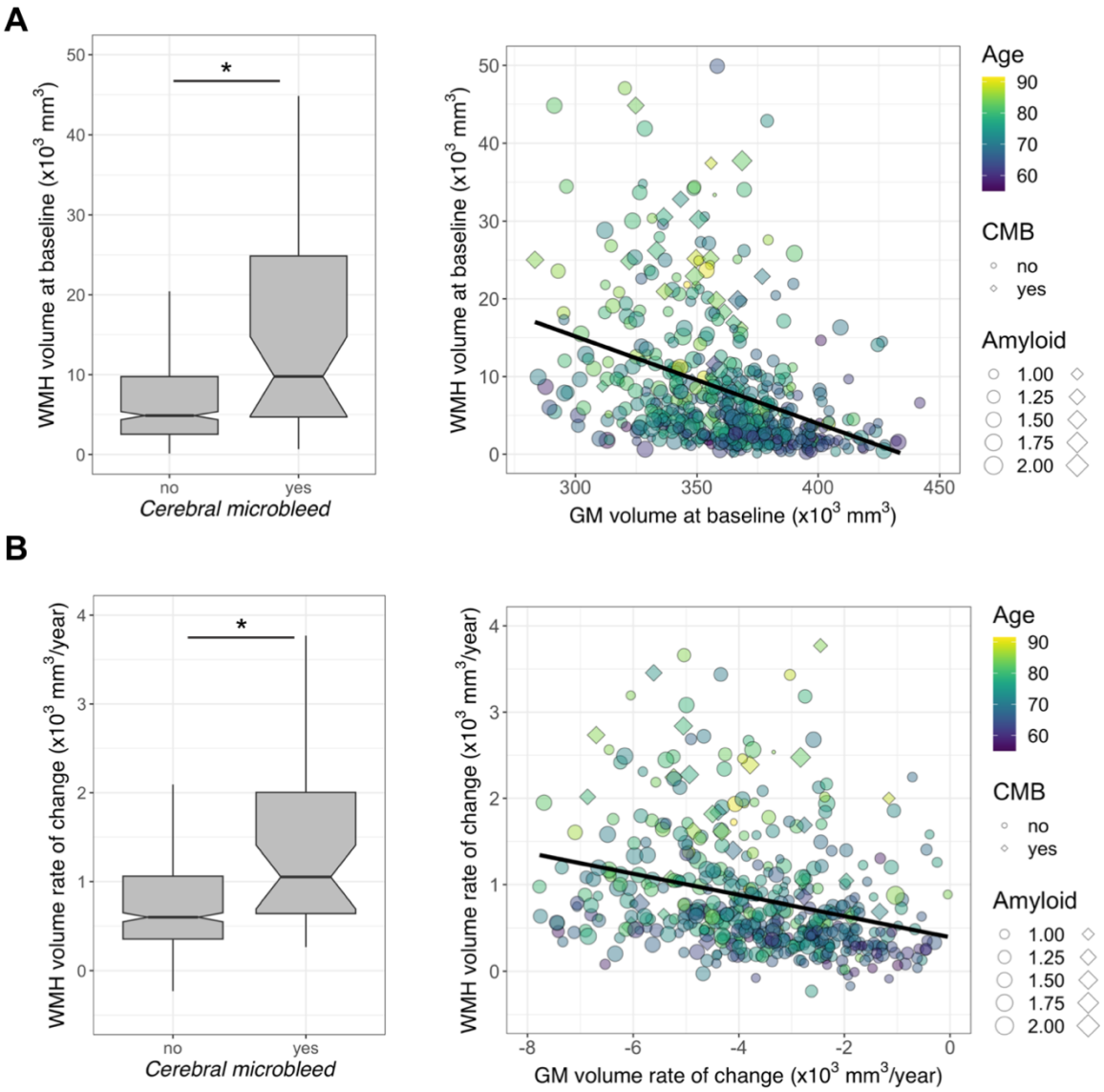

Figure 3: Cerebral microbleeds (CMB) and gray matter (GM) volume are associated with WMH in older adults from ADNI, both at baseline (A) and longitudinally (B). Older adults with CMB were observed to have greater WMH volume at baseline (top left) and had greater rates of longitudinal WMH volume growth (bottom left) compared to those without CMB. In addition, baseline WMH volume was negatively associated with GM volume in ADNI participants (top right). Using longitudinal MRI data from ADNI, we observed WMH volume growth was greater as GM volume declined (bottom right).

**: $p<0.05$*

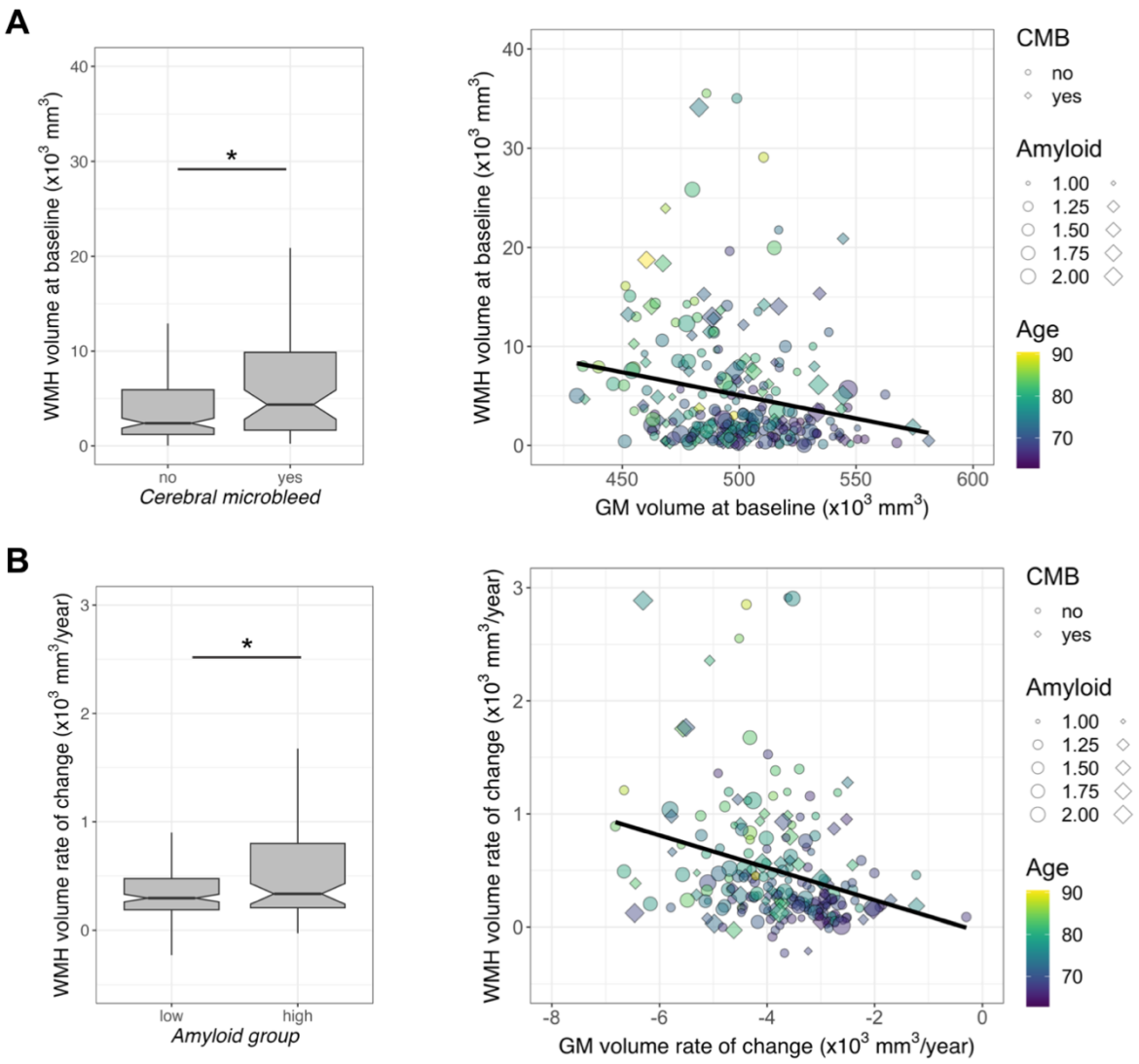

Figure 4: Cerebral microbleeds (CMB) and gray matter (GM) volume are associated with WMH volume in older adults from HABS at baseline. Older adults with CMB were observed to have greater WMH volume at baseline (top left). In addition, baseline WMH volume was negatively associated with GM volume in HABS participants (top right). Using longitudinal MRI data from HABS, we observed WMH volume growth was greater in high amyloid group compared to the lower amyloid group (bottom left) and it was also related to rate of GM volume decline (bottom right).

**: $p<0.05$*

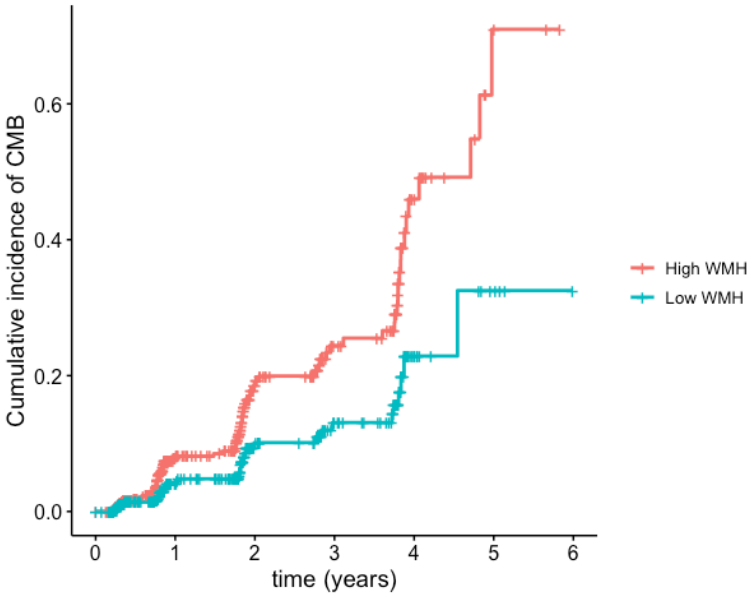

Figure 5: Survival analysis for ADNI participants without CMB at baseline. Among older adults without CMBs at the study baseline, those with WMH higher than the group median (High WMH; salmon color) had a significantly higher probability of developing CMB during longitudinal follow-up (Cox hazard ratio=2.63, $p<0.001$) than those with baseline WMH volume below the group median (Low WMH; teal color).

Supplementary Table 1: Participants' demographics and study information for the DIAN, ADNI, and HABS baseline data for the highest FHS-CVD tertile group. Mean (Standard deviation) or number (percentage) are reported.

	DIAN (N=81)	**ADNI (N=159)**	**HABS (N=93)**
Age (years)	48.5 (8.6)	77.4 (6.5)	77.0 (6.4)
Estimated year to symptom onset (years)	-.5 (8.5)	NA	NA
APOE e4 (yes)	26 (32%)	80 (50%)	22 (24%)
Sex (Female)	24 (30%)	18 (11%)	21 (23%)
Education (years)	14 (3)	16 (3)	15 (3)
Cerebral microbleed (yes)	17 (21)	19 (12%)	31 (34%)
CDR (1+)	48 (60%)	110 (69%)	0 (0%)
Diagnostic group (dementia)	33 (41%)	28 (18%)	0 (0%)
Amyloid group (high)	NA	87 (60%)	43 (46%)
WMH volume (normalized to ICV=1300cm^3)	3.2 (8)	12 (10)	8 (9)
GM volume (normalized to ICV=1300cm^3)	504 (41)	350 (26)	490 (29)
Follow-up time (years)	2 (1.9)	2.8 (2.3)	5.1 (3.7)
FHS-CVD score	10.4 (5.6)	65 (13)	51 (11)
Hypertension (yes)	9 (11%)	111 (70%)	61 (66%)
Hypercholestromia (yes)	17 (21%)	91 (57%)	48 (52%)
Diabetes (yes)	2 (2.5%)	29 (18%)	22 (24%)

Supplementary table 2: Sensitivity analyses using cross-sectional (baseline) DIAN data.

White matter hyperintensities volume ~	**Primary model (r2=.32)**	**Sensitivity analysis 1 (r2=.32)**	**Sensitivity analysis 2 (r2=.46)**
Age	**.35 (.21, .5), t=4.7, p<.001***	**.29 (.1, .49), t=3.0, p=.003***	**.39 (.11, .67), t=2.8, p=.007***
Cerebral microbleed (yes)	**.48 (.04, .93), t=2.1, p=0.03***	.4 (-.06, .86), t=1.7, p=.09	-.01 (-.57, .55), t=-.03, p=.9
Gray matter volume	**-.17 (-.32, -.03), t=-2.3, p=0.02***	**-.17 (-.32, -.02), t=-2.3, p=.02***	**-.45 (-.71, -.19), t=-3.4, p=.001***
Amyloid burden	.08 (-.05, .21), t=1.1, p=.2	.08 (-.05, .21), t=1.2, p=.2	-.01 (-.23, .22), t=.05, p=.9
Framingham Heart Study Cardiovascular Disease risk score	NA	.08 (-.09, .26), t=.9, p=.3	-.08 (-.34, .17), t=-.6, p=.5

Standardized beta values are shown. Positive beta values indicate positive associations.

Sensitivity analysis 1: adding FHS-CVD

Sensitivity analysis 2: the same model of sensitivity analysis 1 in the highest tertile of FHS-CVD

Supplementary table 3: Sensitivity analyses using longitudinal DIAN data.

white matter hyperintensities volume rate of change ~	**Primary model (r2=.5)**	**Sensitivity analysis 1 (r2=.5)**	**Sensitivity analysis 2 (r2=.49)**
Age	**.47 (.33, .6), t=6.8, p<0.001***	**.42 (.24, .61), t=4.5, p<0.001***	**.55 (.23, .86), t=3.5, p=0.001***
Cerebral microbleed	**.65 (.25, 1.1), t=3.2, p=0.001***	**.58 (.17, 1.0), t=2.8, p=0.006***	.12 (-.42,.66), t=.4, p=.6
gray matter volume rate of change	**-.21 (-.34, -.07), t=-3.1, p=0.002***	**-.2 (-.34, -.07), t=-2.9, p=0.003***	**-.37 (-.63, -.1), t=-2.8, p=0.008***
amyloid burden	.07 (-.06,.2), t=1.1, p=.3	.08 (-.05,.21), t=1.2, p=.2	.06 (-.19,.31), t=.5, p=.6
Framingham Heart Study Cardiovascular Disease risk score	NA	.06 (-.11,.24), t=.7, p=.4	-.21 (-.52,.1), t=-1.3, p=.2

Standardized beta values are shown. Positive beta values indicate positive associations.

Sensitivity analysis 1: adding FHS-CVD

Sensitivity analysis 2: the same model of sensitivity analysis 1 in the highest tertile of FHS-CVD

Supplementary table 4: Sensitivity analyses using cross-sectional (baseline) ADNI data.

White matter hyperintensities volume ~	**Primary model (r2=0.34)**	**Sensitivity analysis 1 (r2=0.36)**	**Sensitivity analysis 2 (r2=0.28)**
Age	**.4 (.32, .47), t=10.5, p<.001***	**.38 (.29, .47), t=8.2, p<.001***	**.41 (.25, .56), t=5.1, p<.001***
Cerebral microbleed	**.32 (.04, .6), t=2.3, p=.02***	.23 (-.06, .5), t=1.6, p=.1	.1 (-.4, .58), t=.4, p=.6
Gray matter volume	**-.26 (-.33, -.18), t=-6.8, p<.001***	**-.25 (-.34, -.17), t=-6.1, p<.001***	**-.17 (-.33, -.01), t=-2.1, p=.03***
Amyloid burden (high)	**.16 (.01, .3), t=2.2, p=.03***	.15 (-.01, .3), t=1.9, p=.06	.25 (-.06, .56), t=1.6, p=.1
Framingham Heart Study Cardiovascular Disease risk score	NA	.07 (-.02, .16), t=1.6, p=.1	.01 (-.14, .16), t=0.12, p=.9

Standardized beta values are shown. Positive beta values indicate positive associations.

Sensitivity analysis 1: adding FHS-CVD

Sensitivity analysis 2: the same model of sensitivity analysis 1 in the highest tertile of FHS-CVD

Supplementary table 5: Sensitivity analyses using longitudinal ADNI data.

white matter hyperintensities volume rate of change ~	**Primary model (r2=.27)**	**Sensitivity analysis 1**	**Sensitivity analysis 2 (r2=.24)**
Age	**.35 (.28, .43), t=9.1, p<0.001***	**.34 (.25, .44), t=7.0, p<0.001***	**.34 (.18, .5), t=4.2, p<0.001***
Cerebral microbleed	**.24 (.06, .41), t=2.7, p=0.008***	**.23 (.04, .42), t=2.3, p=0.02***	**.46 (.11, .82), t=2.6, p=0.01***
gray matter volume rate of change	**-.23 (-.31, -.15), t=-5.6, p<0.001***	**-.23 (-.32, -.14), t=-5.0, p<0.001***	**-.31 (-.48, -.14), t=-3.6, p<0.001***
amyloid burden (high)	**.19 (.02, .35), t=2.3, p=.02***	.16 (-.02, .34), t=1.8, p=.07	-.1 (-.47, .26), t=-.5, p=.5
Framingham Heart Study Cardiovascular Disease risk score	NA	.03 (-.06, .12), p=.5	-.09 (-.25, .07), t=-1.1, p=.2

Standardized beta values are shown. Positive beta values indicate positive associations.

Sensitivity analysis 1: adding FHS-CVD

Sensitivity analysis 2: the same model of sensitivity analysis 1 in the highest tertile of FHS-CVD

Supplementary table 6: Sensitivity analyses using cross-sectional (baseline) HABS data.

White matter hyperintensities volume ~	**Primary model (r2=0.21)**	**Sensitivity analysis 1 (r2=0.24)**	**Sensitivity analysis 2 (r2=0.3)**
Age	**.34 (.22, .46), t=5.4, p<.001***	**.34 (.21, .48), t=5.0, p<.001***	**.46 (.27, .66), t=4.7, p<.001***
Cerebral microbleed	**0.28 (.03,.53), t=2.2, p=.02***	0.16 (-.1,.4), t=1.2, p=.2	.06 (-.3, .5), t= .3, p=.8
Gray matter volume*amyloid burden [high]	**-.23 (-.45, -.01), t=-2.1, p=.04***	**-.27 (-.5, -.04), t=-2.4, p=.01***	-.2 (-.6, .1), t=-1.3, p=.2
Framingham Heart Study Cardiovascular Disease risk score	NA	0.1 (-.02,.23), t=1.6, p=.1	.03 (-.2,.2), t= .3, p=.8

Standardized beta values are shown. Positive beta values indicate positive associations.

Sensitivity analysis 1: adding FHS-CVD

Sensitivity analysis 2: the same model of sensitivity analysis 1 in the highest tertile of FHS-CVD

As a significant gray matter volume by amyloid group interaction was observed in HABS analyses, this term was retained in statistical models.

Supplementary table 7: Sensitivity analyses using longitudinal HABS data.

White matter hyperintensities volume rate of change~	**Primary model (r2=0.18)**	**Sensitivity analysis 1 (r2=0.19)**	**Sensitivity analysis 2 (r2=0.23)**
Age	**.34 (.21, .46), t=5.4, p<.001***	**.26 (.11, .4), t=3.4, p=.001***	**.32 (.1, .55), t=2.8, p=.006***
Gray matter volume rate of change*amyloid burden[high]	**-.27 (-.51, -.03), t=-2.2, p=.03***	**-.30 (-.55, -.04), t=-2.3, p=.02***	-.13 (-.6, .3), t=-.6, p=.5
Framingham Heart Study Cardiovascular Disease risk score	NA	0.13 (-.01,.27), t=1.8, p=.06	.02 (-.2,.23), t= .2, p=.8

Standardized beta values are shown. Positive beta values indicate positive associations.

Sensitivity analysis 1: adding FHS-CVD

Sensitivity analysis 2: the same model of sensitivity analysis 1 in the highest tertile of FHS-CVD

As a significant gray matter volume by amyloid group interaction was observed in HABS analyses, this term was retained in statistical models. Longitudinal CMB data was not available in HABS participants.

Supplementary Table 8: Sample characteristics for ADNI Participants without baseline CMB.

	CMB emergent (n=100)	CMB negative (n=427)
Age (years)	73.3 (7.0)	72.2 (7.2)
Sex (Female)	49 (49%)	210 (49%)
APOE e4 (yes)	52 (52%)	192 (45%)
Education (years)	16 (3)	16 (3)
WMH volume	10 (10)	8 (8)
GM volume	364 (26)	359 (31)
Diagnostic group (dementia)	8 (8%)	57 (13%)
Amyloid group	49 (49%)	192 (47%)
Framingham Heart Study Cardiovascular Disease risk score	38 (22)	37 (22)
Clinical dementia rating (1+)	59 (59%)	238 (56%)
Follow-up time (years)	4.8 (2.8)	3.5 (2.7)
Number of sessions	3.6 (1.3)	3.5 (1.3)